

## Least-squares migration with gathers

A.A. Valenciano\*, M. Orlovich, E. Klochikhina and N. Chemingui, PGS

### Summary

Least-Squares Migration (LSM) reduces the amplitude variations due to uneven illumination and migration operator restrictions. When posed as an inversion in the angle domain, LSM compensates the angle gather amplitudes and improves their resolution. Our LSM angle extension requires an explicit computation of the Hessian matrix or Point Spread Functions (PSFs). The algorithm applies a chain of operators and their adjoints for modeling, migration, and offset to angle transformation to a grid of point scatterers distributed through the model. It effectively incorporates the spatial and angle variability of the PSF. The angular reflectivity is recovered by solving a linear system of equations that deconvolves the multidimensional PSF from the migrated image gathers. Results from the Sigsbee model and a multisensor streamer survey acquired in the Central North Sea show how LSM improves the image resolution and Amplitude Versus Angle (AVA) reliability.

### Introduction

Earth models, acquisition parameters, and imaging operators affect seismic amplitudes. The bias is particularly prominent in the presence of complex models, impacting the interpretation of amplitudes variability with angle. Provided with an accurate velocity model, migration produces flat angle gathers. Abrupt changes in amplitude with angle are typically indicative of illumination problems. Furthermore, depth-imaging operators (i.e. modeling /migration) are non-unitary (Claerbout, 1992). If  $L$  is a modeling operator, and  $L'$  is its adjoint (migration), their product  $H=L'L$  is not the identity matrix.  $H$  is a Hessian matrix, whose elements are the point spread functions (PSF). As a result, depth migrated images are blurred, and their AVA fidelity is often not preserved.

The severity of the distortion depends on the migration operators. Wave equation one-way (WEM), two-way (RTM) or asymptotic (Kirchhoff) handle the amplitudes differently and have different degrees of kinematic accuracy (Gray et al., 2001; Zhang et al., 2005). Asymptotic Kirchhoff operators are closer to unitary (Bleistein, 1987) and are often the preferred choice for AVA interpretation, in spite of their kinematic limitations in high-contrast and rapidly varying earth models. As Full Waveform Inversion (FWI) increases our ability to estimate more detailed earth models (Figure 1), there is an increased demand for the more kinematically accurate wave-equation operators that could also preserve the migrated image amplitudes.

Here, we propose a wave-equation LSM solution that reduces the image blurring and corrects the amplitude errors in angle-domain common image gathers. The algorithm assumes that the background earth model is accurate and poses the estimation of the reflectivity as a linear inversion problem in the reflection angle domain. It explicitly computes the Hessian matrix with an angle dimension by applying a sequence of operators (modeling/migration and offset to angle transforms) to a grid of point scatterers. The method assumes a degree of stationarity of the PSFs as they are later interpolated to fully populate the image space. The final step solves a linear system where the migrated images and the PSFs are the known quantities, and the angular reflectivity is the unknown. Results from the Sigsbee model and a multisensor field survey from the central North Sea demonstrate the benefits of the inversion approach.

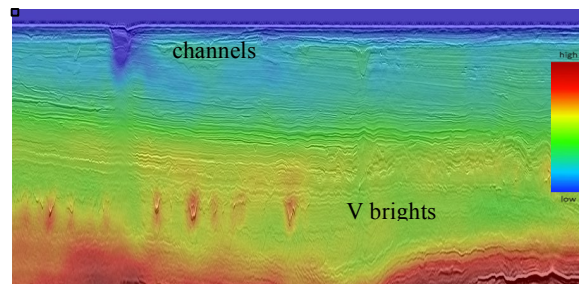


Figure 1 Velocity model from the Central North Sea Viking Graben derived using FWI.

### Least-squares Migration with gathers

The LSM algorithm can be summarized as follows: given a linear modeling operator  $L$  and a reflectivity model  $m$ , compute synthetic data  $d$  using the relation  $d = Lm$ , then form a quadratic cost function

$$S(\mathbf{m}) = \|\mathbf{d} - \mathbf{d}_{obs}\| = \|\mathbf{Lm} - \mathbf{d}_{obs}\|, \quad (1)$$

where  $\mathbf{d}_{obs}$  is the field data, and we seek a reflectivity model  $\mathbf{m}$  that minimizes it.

A closed form solution for the least-squares estimate of  $m$  is given by:

$$\hat{\mathbf{m}} = (\mathbf{L}'\mathbf{L})^{-1} \mathbf{L}'\mathbf{d}_{obs} \quad (2)$$

$$\hat{\mathbf{m}} = \mathbf{H}^{-1} \mathbf{m}_{mig}, \quad (3)$$

where the migration operator  $\mathbf{L}'$  is the adjoint of the modeling operator  $\mathbf{L}$ ,  $\mathbf{m}_{mig}$  is the migrated image, and  $\mathbf{H}$  is

## Least-squares migration with gathers

the Hessian matrix whose elements are the PSFs. Equation 3 implies that the reflectivity can be estimated by a matrix-vector multiplication of the inverse of the Hessian ( $\mathbf{H}^{-1}$ ) by the migrated image ( $\mathbf{m}_{mig}$ ). However, it is not numerically feasible to compute the inverse Hessian matrix for most field data applications. Alternately, a low-rank approximation to the inverse of the Hessian has been proposed (e.g. Guitton, 2004).

A better approach is to explicitly compute the Hessian matrix and estimate the reflectivity (Valenciano, 2008) rather than approximating the matrix inverse. This solution is obtained by solving the linear system:

$$\mathbf{H}\hat{\mathbf{m}} = \mathbf{m}_{mig}, \quad (4)$$

using an iterative inversion algorithm (e.g. conjugate gradients). To generalize equation 4, and invert for angular reflectivity, we need to define the Hessian in the prestack image space.

### Expanding Hessian dimensionality to the angle domain

Valenciano and Biondi (2006) defined the Hessian matrix in the prestack image domain as a chain of operators from the subsurface offset  $\mathbf{h} = (h_x, h_y)$  to the reflection and azimuth angle  $\Theta = (\theta, \alpha)$ :

$$\mathbf{H}(\mathbf{x}, \Theta, \mathbf{x}', \Theta') = \mathbf{T}'(\Theta, \mathbf{h}) \mathbf{H}(\mathbf{x}, \mathbf{h}, \mathbf{x}', \mathbf{h}') \mathbf{T}(\Theta', \mathbf{h}') \quad (5)$$

where the operator  $\mathbf{T}$  defines the transformation from reflection and azimuth angle to subsurface offset (Sava and Fomel, 2003). The approach of Valenciano and Biondi (2006) can be applied to any prestack volume where angle gathers are produced from direct binning using Poynting Vectors (Yoon and Marfurt, 2006) or extended imaging conditions (Sava and Fomel, 2005). After computing the angle domain Hessian, the linear system from equation 4 can be expanded to estimate the least-squares angular reflectivity (Valenciano 2008):

$$\mathbf{H}(\mathbf{x}, \Theta, \mathbf{x}', \Theta') \hat{\mathbf{m}}(\mathbf{x}, \Theta) = \mathbf{m}_{mig}(\mathbf{x}, \Theta). \quad (6)$$

Here, we compute the Hessian matrix in the angle domain by applying the sequence of operators from equation 5 to a grid of point scatterers distributed throughout the model space. The spacing of the point scatterers is controlled by the acquisition geometry, medium velocity, and imaging frequency.

### The Sigsbee model

The Sigsbee model (Figure 2) is ideal for illustrating the variable illumination on angle gathers (Figure 3 and Figure 4). Note how angle illumination remains uniform in the sediments but dramatically changes below salt (Figure 3a and 3b). Also note the changes in the PSFs with angle (4

vs. 24 degrees) in Figures 4a and 4b. They indicate that not only the amplitudes change, but also the angle resolution changes rapidly under the salt body.

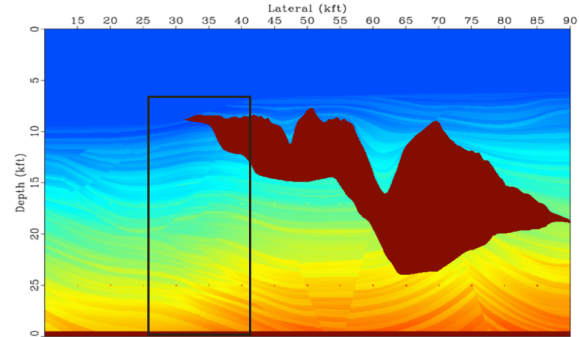


Figure 2 Sigsbee velocity model.

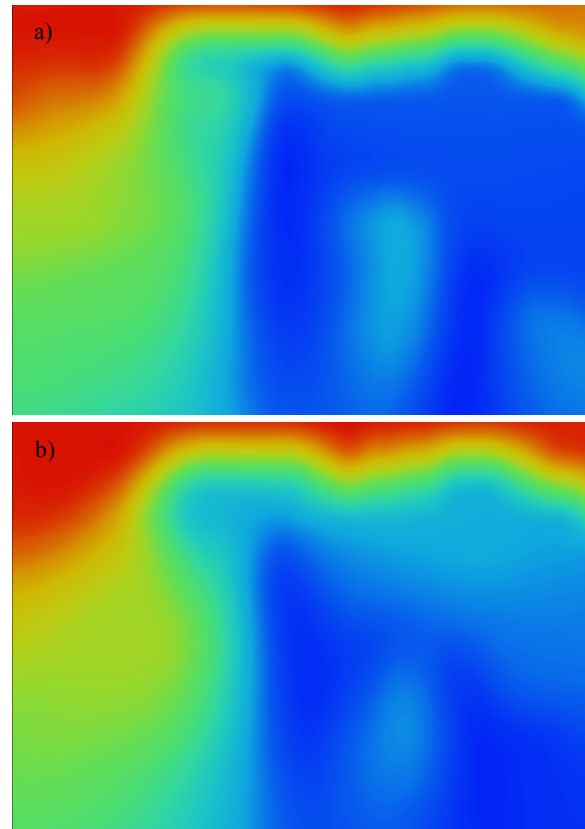


Figure 3 Sigsbee model, common angle illumination: a) illumination at 4 degrees, b) illumination at 24 degrees.

We generated synthetic data with constant amplitude angle gathers (i.e. no AVA). As expected, the migration (WEM) angle gathers (Figure 5a) show uneven illumination; noticeably under the salt. In contrast, the LSM angle gathers (Figure 5b) show the expected AVA response in the

## Least-squares migration with gathers

sediments, and less variability than the conventional migration below the salt.

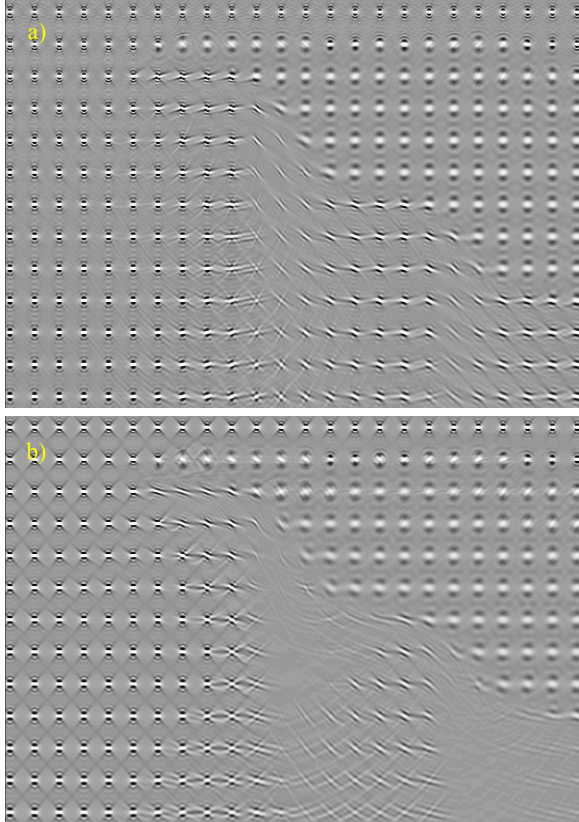


Figure 4 Sigsbee model, common angle PSFs: a) PSFs at 4 degrees, and b) PSFs at 24 degrees.

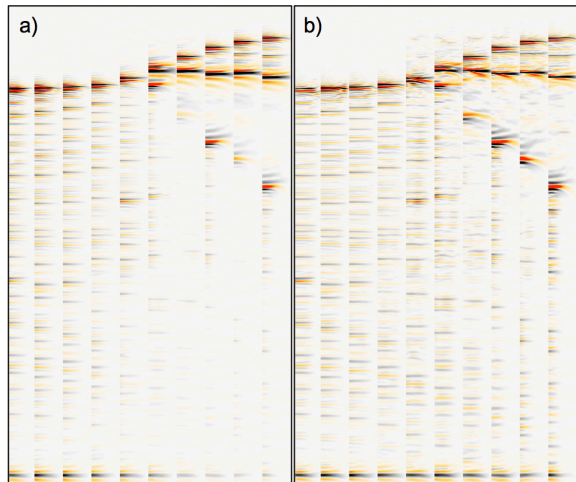


Figure 5 Sigsbee angle gathers (extracted in the rectangular area in Figure 2): a) migration, and b) LSM.

### Field data from the North Sea

We used a 3D narrow-azimuth multisensor streamer dataset from the Central North Sea (Viking Graben) to further illustrate the advantages of LSM. There a complex overburden, with high-velocity bodies (“V bright”) and shallow low velocity channels (Figure 1), produces uneven illumination at the reservoir level. Figures 6 and 7 show a comparison of the stacked images from both the migration (WEM) and LSM. The LSM improves resolution, enabling a better discrimination of the reservoir from the background. Figures 8 and 9 show angle gathers at the target and their corresponding AVA response. The illumination compensation with LSM changes the AVA trend as well as the interpretation at the reservoir (Figure 9). The LSM AVA trend matches the response predicted by AVA modeling from a nearby well.

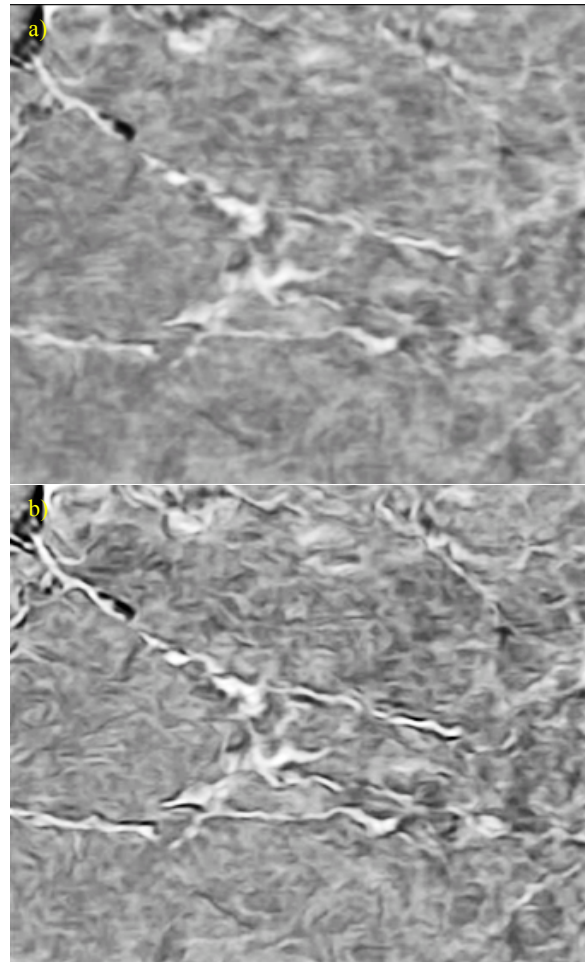


Figure 6 Central North Sea data depth slice (1.8 km) of the angle stacked images: a) Migration, and b) LSM.



## Least-squares migration with gathers

### Conclusions

Least-Squares Migration (LSM) produces high-resolution images ready for reservoir characterization. Our wave equation LSM solution creates reliable AVA responses in complex media. Synthetic and field data examples show improvement after LSM in image resolution and AVA consistency. On the data from the Central North Sea, the LSM illumination compensation changed the AVA interpretation at the reservoir level. We conclude that LSM is a robust solution, producing volumes of angular reflectivity for AVA attributes analysis.

### Acknowledgments

We thank PGS MultiClient for permission to use the field data. We also thank AkerBP for the interpretation insights. We appreciate the assistance of Øystein Korsmo to make the field data available and for fruitful discussions

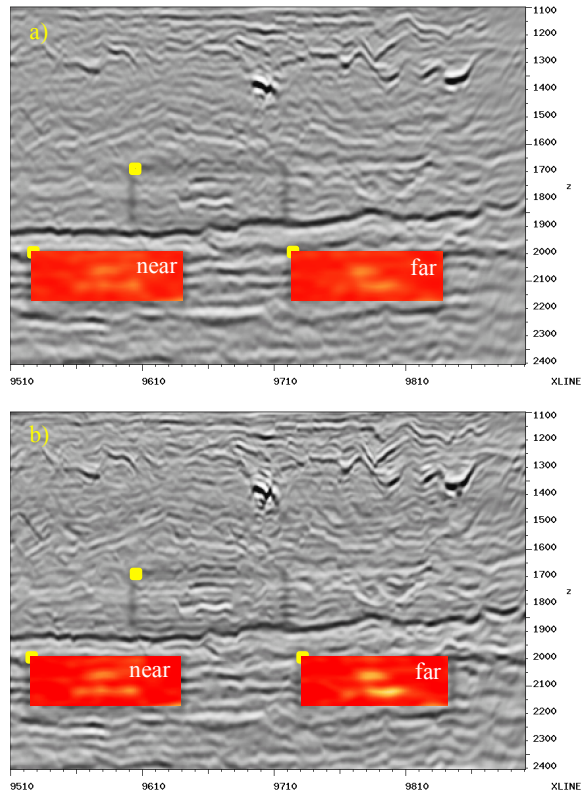


Figure 7 Central North Sea data inline of the angle stacked inline section: a) Migration, b) LSM. The yellow rectangle is centered at the reservoir. The RMS absolute amplitudes of the near vs. the far angle stacks are displayed inside the highlighted area. Note how the LSM allows for better discrimination of the reservoir from the background.

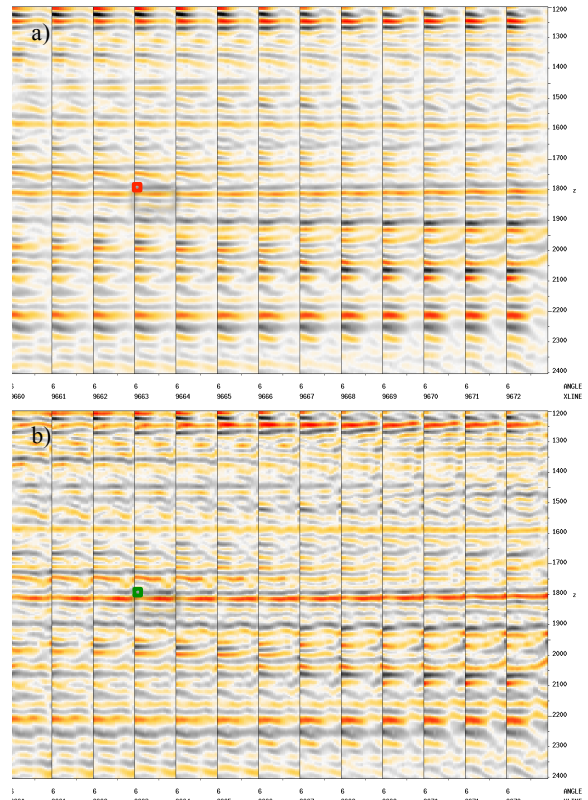


Figure 8 Central North Sea data angle gathers from 4 to 36 degrees: a) Migration and b) LSM.

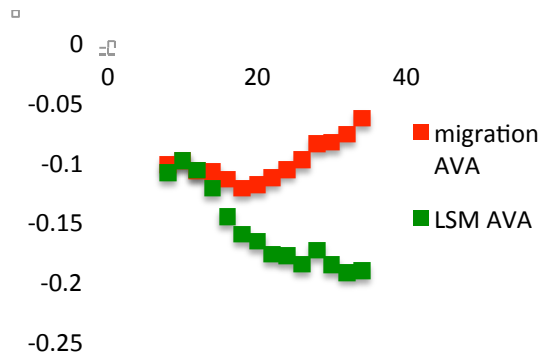


Figure 9 Central North Sea data: AVA comparison at the reservoir depth (read and green rectangles in Figure 8). The illumination compensation with LSM changes the AVA trend.

## REFERENCES

- Bleistein, N., 1987, On the imaging of reflectors in the earth: *Geophysics*, **52**, 931–942, doi: <https://doi.org/10.1190/1.1442363>.
- Claerbout, J. F., 1992, *Earth soundings analysis: Processing versus inversion*: Blackwell Scientific Publications.
- Gray, S. H., J., Etgen, J., Dellinger, and D., Whitmore, 2001, Seismic migration problems and solutions: *Geophysics*, **66**, 1622–1640, doi: <https://doi.org/10.1190/1.1487107>.
- Guitton, A., 2004, Amplitude and kinematic corrections of migrated images for nonunitary imaging operators: *Geophysics*, **69**, 1017–1024, doi: <https://doi.org/10.1190/1.1778244>.
- Sava, P., and S., Fomel, 2003, Angle-domain common-image gathers by wavefield continuation methods: *Geophysics*, **68**, 1065–1074, doi: <https://doi.org/10.1190/1.1581078>.
- Sava, P., and S., Fomel, 2005, Time-shift imaging condition: 75th Annual International Meeting, SEG, Expanded Abstracts, 1850–1853, doi: <https://doi.org/10.1190/1.2148063>.
- Valenciano, A. A., and B. L., Biondi, 2006, Wave-equation angle-domain Hessian: 68th Annual International Conference and Exhibition, EAGE, Expanded Abstracts, G042, doi: <https://doi.org/10.3997/2214-4609.201402166>.
- Valenciano, A.A., 2008, *Imaging by wave-equation inversion*: Ph.D. thesis, Stanford University.
- Yoon, K., and K. J., Marfurt, 2006, Reverse-time migration using the Poynting vector: *Exploration Geophysics*, **37**, 102–107, doi: <https://doi.org/10.1071/EG06102>.
- Zhang, Y., G., Zhang, and N., Bleistein, 2005, Theory of true-amplitude one-way wave equations and true-amplitude common-shot migration: *Geophysics*, **70**, no. 4, E1–E10, doi: <https://doi.org/10.1190/1.1988182>.